Fiber-coupled single ion as an efficient quantum light source

Alex Wilson, Hiroki Takahashi, Andrew Riley-Watson, Fedja Oručević, Peter Blythe, Anders Mortensen,
Daniel R. Crick, Nicolas Seymour-Smith, Elisabeth Brama, Matthias Keller, and Wolfgang Lange*
Department of Physics and Astronomy, University of Sussex, Brighton, BN1 9QH, United Kingdom
(Dated: January 26,2011)

We have realized a compact system to efficiently couple the fluorescent light emitted by a single trapped ion to two opposing optical fibers. The fibers are tightly integrated in the center electrodes of a miniature endcap trap. They capture light from the ion with a numerical aperture of 0.34 each, corresponding to 6% of the solid angle in total. The high collection efficiency and high signal-to-background ratio make the setup an ideal quantum light source. We have observed strong antibunching of the photons emitted from the two fibers. The system has a range of applications from single-ion state detection in quantum information processing to strong coupling cavity-QED with ions.

The interaction of light and single atomic particles has evolved from a subject of fundamental interest to a unique tool for modern quantum technology. The fluorescent radiation emitted by single atoms has pronounced quantum properties, as demonstrated by the second order correlation function [1]. While early experiments provided little control over individual atomic particles, advances in trapping and cooling of atoms and ions have led to a range of applications, most notably atom chips and quantum information processing in strings of ions.

An important figure of merit of these systems is the efficiency with which radiation emitted by a single particle is detected. In atom chips, this is essential for the ability to detect the presence of atoms [2]. In ion traps, more efficient collection of fluorescent light speeds up quantum state discrimination, as required for the read-out of a quantum register [3].

As a prerequisite for efficient detection, a high numerical aperture (NA) system must be employed for collecting radiation. The ideal collection efficiency would be achieved if photons from the full solid angle were captured. Recently, 64% of the emission of freely falling atoms was collected by combining two mirrors [4]. There are proposals to approach 100% capture efficiency by surrounding a single atom with a parabolic mirror [5]. In experiments with single ions, the need for trap electrodes and laser access requires a more open structure. Collection efficiencies of 10% have been reached with a spherical mirror integrated with a linear Paul trap [6]. Another approach is to surround the particle with a pair of lenses with large NA [7].

In systems with large optical elements, the geometry of trap and vacuum chamber poses limitations for light detection. A novel way of capturing fluorescence is provided by optical fibers. While the diameter of the fiber core is only on the order of 100 μm, the fiber ends can be brought in close proximity to the fluorescing particle to maximize the numerical aperture. Integrated fibers have been used successfully to detect the presence of atoms on a chip, either in absorption [8] or fluorescence [9]. Even tighter integration of fluorescence collection on atom chips has been proposed by using optical waveguides [10].

Using optical fibers for collecting fluorescence from trapped *ions* is complicated by the fact that the trapping potential is adversely affected by the presence of dielectrics. Proper shielding and tight integration of the fiber in the trapping structure is required [11]. We have realized a novel system for combining optical fibers with an rf ion-trap. It fulfills the requirements of close proximity of the fiber ends to the ion, but at the same time negligible distortion of the trapping field. Our trap design is of the endcap type [12], in which a single ion is stored between the ends of two opposing metal rods connected to an rf-source. Additional hollow coaxial electrodes at rf-ground, surrounding the central electrodes, increase the depth of the trapping potential. The cylindrical symmetry of the trap provides a natural way of combining it with optical fibers. By replacing the central rf-rods with hollow tubes, optical fibers can be inserted in both electrodes [Fig. 1(a)]. The fibers are not flush with the end of the tube, but retracted by 50 μm, so that rf-shielding inside the tube makes the overlap of the dielectric fibers and the rf-field negligible. In addition, the presence of the fibers does not change the cylindrical symmetry of the trap, limiting distortion of the trapping field.

The outer diameter of the central electrodes is 458 μm, the inner diameter 254 μm, and the vertical distance between the electrodes is 446 μm. The optical fiber in our experiment is a Thorlabs BFH48-200 multimode fiber with a core diameter of 200 μm and a NA of 0.48. The hard cladding diameter is 230 μm so that the fiber can be run down the center electrodes with the coating stripped. After inserting the fibers from the back of the electrodes and positioning their end-facets, we fixed them by slightly squeezing the rear of the rf-electrodes. At an ion-fiber separation of 275 μm, the effective NA of the fiber core is 0.34. At this setting, the two fibers combined capture 6% of the full solid angle, only limited by the geometry. The capture efficiency of our setup is approximately twice of what has been demonstrated so far for fibers integrated with ion traps [11]. Using the full numerical
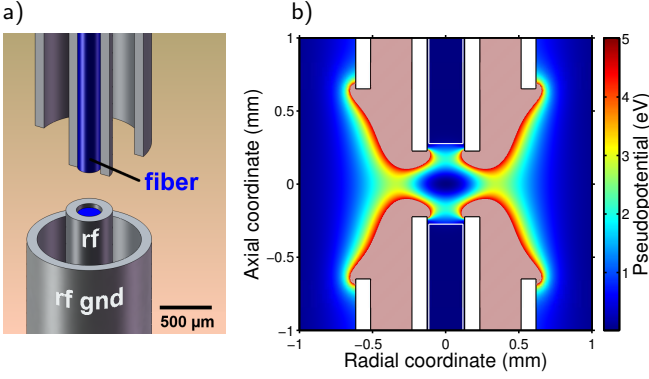
FIG. 1. (color online). (a) Endcap trap with integrated optical fibers. Half of the upper electrode structure is cut away to reveal the upper fiber. (b) Cross-section of the pseudopotential of the trap with fiber, obtained from a finite element calculation by averaging the potential over one rf-cycle.

FIG. 2. (color online). Scheme of the relevant transitions in ^{40}Ca$^+$. We probe the quantum properties of light scattered on the resonance transition at 397 nm (bold arrows). Population trapping due to decay to the D-states is avoided by repumping via the upper P-state (thin arrows).

aperture of the fiber, a capture efficiency of 12.3% can be achieved at an ion-fiber separation of 183 μm.

Calcium ions are loaded from an effusive oven mounted to the side of the trap. To reduce coating of the trap electrodes with calcium, the atomic beam is collimated by means of a tube of inner diameter 250 μm, 2.45 mm away from the center of the trap. The atoms are photoionized using a resonant laser at 423 nm and a second stage at 375 nm for the actual ionization [13]. Once captured in the trapping potential, a single ion is stored for several hours. Compared to an endcap trap with solid central electrodes, tubular electrodes generate a pseudopotential with a 25% lower trap depth [Fig 1(b)]. For an rf-amplitude of 200 V, the calculated potential barriers are 2.8 eV in the radial and 2.1 eV in the axial direction. The secular frequencies were measured to be $\omega_r = (2\pi)1.9$ MHz and $\omega_z = (2\pi)3.8$ MHz for a drive frequency of 14.9 MHz.

With a view to applications in spectroscopy, quantum information processing and cavity-QED, the localization of the ion in the trap is of particular importance. As a first step, the ion is laser-cooled on the $S_{1/2} \to P_{1/2}$ transition with a wavelength of λ=397 nm. Lasers with a power of several μW are injected from the side under different angles, red-detuned by roughly half the linewidth $\Gamma=(2\pi)22.3$ MHz. To avoid optical pumping to the $D_{3/2}$ and the $D_{5/2}$ level, we apply lasers at 850 nm and and 854 nm, returning the ion to the ground state via the $P_{3/2}$-level [Fig 2].

The ion may also undergo a periodic oscillation, driven by the rf-trapping field (micromotion), if dc electric stray fields push the ion off the central node of the rf-field. In order to minimize micromotion, we compensate stray fields by applying voltages to a set of compensation electrodes. The atomic beam collimator serves as the electrode compensating dc stray fields in the direction of the oven. Horizontal dc-fields orthogonal to the oven are compensated via a small wire mounted to the side, while a vertical dc offset-field can be applied via the rf-ground
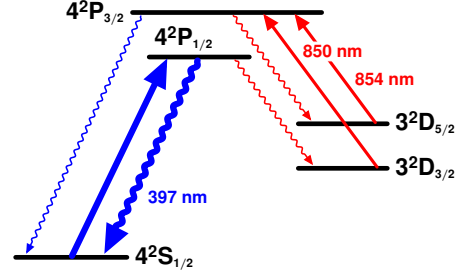
electrodes. With the help of these electrodes, we position the ion at the rf-center of the trap, where its micromotion is minimal. The required dc-voltages are determined by probing the rf-modulation of the fluorescence intensity using UV pump-beams in three non-collinear directions.

The ion's localization that can be achieved depends on the sensitivity with which we detect micromotion. The sensitivity to Doppler modulation in our experiment is $0.016\Gamma/\sqrt{\text{Hz}}$. For an acquisition time of 4 s, we can detect an axial displacement of $0.006\Gamma\lambda/\omega_z \approx 0.04\lambda$. Therefore, by compensating stray fields and nulling the micromotion, we localize the ion in a region smaller than the wavelength (Lamb-Dicke regime), a fact which is essential for applications in cavity-QED.

The presence of the fiber facets close to the ion might potentially lead to stray electric fields at the position of the ion due to the accumulation of charges on dielectric surfaces [14, 15]. If left uncompensated, the ion would be pushed off the rf-node and hence become subject to micromotion, resulting in line broadening and reduced coupling to light. Charges might be created by direct laser-illumination of surfaces or in the photoionization of atomic calcium. We minimize these effects by reducing the beam waists and recessing the end of the fibers as described above. Another source of stray fields are contact potentials in sections of the electrodes partially coated with calcium.

As a sensitive probe for the presence of stray fields, we have utilized the trapped ion itself. Automatically nulling the micromotion at intervals of 2 minutes, we tracked the compensation voltages over time after loading the trap. Using a model of the trap fields obtained from a 3D finite element calculation, the compensation voltages are converted to an electric field at the center of the trap which must be equal and diametrically opposed to the instantaneous stray field. The sensitivity of the measurement was 60 mV/(cm$\sqrt{\text{Hz}}$). Our data showed stationary conditions during normal operation of the trap. Immediately after loading, stray fields on the order of 1 V/cm appear, but decay exponentially at a rate of 5×10^{-4}s^{-1} on average. Since we measure all

three spatial components of the electric field, we can locate where it originates from. We find that the sources lie in a small azimuthal segment on the edge of the central rf-electrodes, on the side facing the oven. There is no evidence of fields from the direction of the fibers. This is a strong indication that charging of the fiber end-facets does not play a major role, but that patch potentials on the electrodes are responsible.

In order to distinguish between the effects of laser illumination and the atomic beam, we switched the photoionization lasers and oven on individually, then observed the effect on an ion already present in the trap. The atomic beam on its own did not affect the micromotion of the ion. Laser illumination at 423 nm and 375 nm alone lead to a change in compensation voltages, but it was a factor of 30 smaller than after loading the trap. This resilience to charging is further evidence for the compatibility of optical fibers with our trap setup.

With the trapped ion centered between the fiber ends and the fluorescent light captured and guided to the detectors by optical fibers, there is no need for additional optics or any optical alignment, making the setup very easy to maintain. Both fibers are connected to atmosphere via vacuum feedthroughs (core diameter 400 μm) which in turn are linked to photomultiplier tubes (PMT, Hamamatsu H5773) by another optical fiber (core diameter 600 μm). Total transmission is approximately 80%. We have investigated the quantum properties of light emitted on the $P_{1/2} \to S_{1/2}$ transition [Fig. 2]. The small dimensions of the trap require special care to prevent stray light from entering the optical fibers and reducing the signal-to-background ratio (SBR). In order to minimize scattered light, we spatially filter the principal 397 nm beam and focus it with a diffraction limited lens (NA=0.25). In this way, we strongly suppress the background count rate in both channels.

Spectroscopy with fiber-based fluorescence detection is demonstrated by scanning the 397 nm laser over the red-detuned half of the resonance line of the calcium ion, where laser-cooling occurs. Combining the signal from both fibers, we measur a peak fluorescence count rate of 36k counts per second (cps) at the saturation intensity (I_s) against a background of 740 cps due to stray light and PMT dark counts. This corresponds to a SBR of 49. At slightly higher laser intensities, count rates up to 55 kpcs are observed [Fig 3]. Thus, the combination of endcap-trap and optical fibers provides excellent conditions for spectroscopy of a single ion.

It is well known that the fluorescent light of a single atomic emitter has non-classical characteristics. They can be probed via the photon statistics which shows perfect antibunching [16]. Antibunched fluorescence from a single atom was first demonstrated in an atomic beam [1] and later with ions [17]. The fact that the second order correlation function is close to zero at times smaller than the relaxation time of the transition can be interpreted as the emission of photons one by one, separated
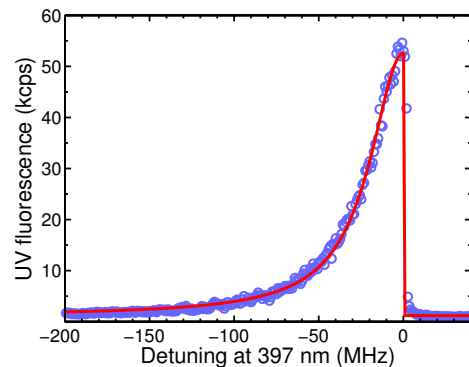

FIG. 3. (color online). Fluorescence spectrum of a single ion in the fiber-coupled endcap trap. Excitation and repumping beams at a power of 0.39 μW (equivalent to an intensity of $1.3I_s$) and 0.5 mW, respectively, are injected from the side of the trap. The combined fluorescence of the two fibers is plotted and no background subtracted. It is fit by a Lorentzian with a half width of 23.8 MHz (solid line).

by the required atomic repumping. This makes a single driven ion an efficient source of single photons, even though emission occurs at random times.

The fiber-coupled endcap trap allows us to directly investigate the quantum properties of the fluorescent light from a single ion. Each of the two fibers delivers an antibunched stream of photons. Even more importantly, the arrival times of photons in the two fibers are anticorrelated, as they originate from the same single ion. Our setup is an ideal, miniaturized version of the Hanbury-Brown Twiss experiment. Instead of generating two anticorrelated photon streams with the help of a beam splitter down the optical path, we use the photons captured by the two optical fibers directly.

We measure second order correlations between photons in the two fibers by sending the PMT-output to a time-to-digital converter (TDC, FAST 7072T). The device has two separate start and stop channels, which we set up so that photons from each fiber can trigger a correlation measurement, to be stopped by a photon from the other fiber. In this way, we are able to evaluate cross-correlations of all registered photon pulses. A delay of 200 ns in each stop-channel gives us access to positive and negative correlation times. Finally, the two TDC traces are aligned at $\tau = 0$ and added. Figure 4 shows a correlation measurement acquired in 40 minutes, with the driving laser red-detuned by 6 MHz and at a power of 0.16 μW. The signal-to-background ratio in the two fiber channels is $SBR_1 = 75$ and $SBR_2 = 26$, respectively. The difference between them is due to a slight angle of the pump beam, scattering different amounts of light into the upper and lower fibers. The background contribution leads to an offset of 0.05 in the normalized correlation function $g^{(2)}(\tau)$ [see Fig. 4]. After subtracting this offset, we obtain $g^{(2)}(0) = 0.05 \pm 0.04$, an important figure of merit attesting to the quality of our system as a single-photon source. The measured correlation func-
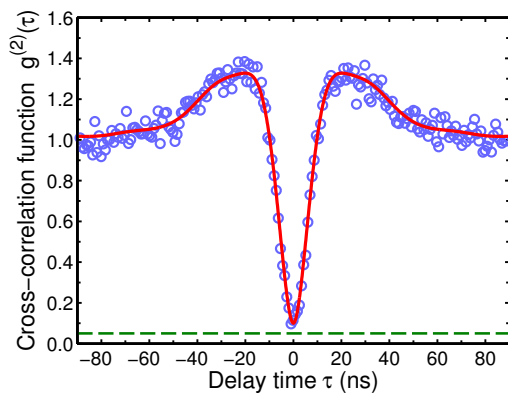
FIG. 4. (color online). Normalized cross-correlation signal $g^{(2)}(\tau)$ of photon arrival times at the end of the two fibers. The dashed line indicates the expected background level due to stray light and dark counts, which have not been subtracted. The excellent agreement with the superimposed numerical solution of the master equation demonstrates the distinct quantum character of the emitted radiation.

tion is in excellent agreement with the solution of the full master equation of the calcium ion, obtained numerically and also shown in Fig 4.

The geometry of a single ion between two opposing optical fibers has important applications beyond efficient state-detection, spectroscopy and the generation of non-classical radiation. By furnishing one or both end-facets of the fibers with a concave surface and providing them with a high-reflectivity coating, an optical resonator can be established, known as a fiber-cavity [18]. A radius of curvature around 100 μm is readily achieved using ablation with a high-power laser. The small separation between the end-facets and the small radius of curvature lead to a very small volume of the cavity modes and hence to strong coupling between the electromagnetic field and an ion inside the cavity. The high stability and long trapping times achieved with single ions make it very attractive to strongly couple them to the field of a fiber-cavity. The endcap-trap geometry implemented here is an ideal way of avoiding the fundamental problem of dielectric materials distorting the rf-trapping field. Our results show that reliable storage of a single ion is possible in the proximity of optical fibers. Finally, note that the architecture of two optical fibers coupled to an ion is ideally suited for the realization of an ion-based quantum repeater [19].

In summary, we have captured the fluorescence of a single ion trapped in an endcap trap, using a pair of optical fibers integrated inside the two central rf-electrodes. Connecting each fiber to a photomultiplier tube provided us with a highly efficient detection system which is easy to maintain, as no optical adjustments are required. The solid angle subtended by the two fibers is 6% of 4π, making it the most efficient fiber detection system implemented for ions so far. We have analyzed the photon statistics of the light emitted by a single ion and have

observed distinct non-classical properties of the radiation, again without any additional optical elements in the setup. The high signal-to-background ratio of 49 leads to a strong antibunching signal. The geometry of the system is identical to that required for coupling a single ion to an optical fiber-cavity and our results show unequivocally that it is technically feasible to provide stable trapping of a single ion in such a setup.

————————

* W.Lange@sussex.ac.uk
[1] H. J. Kimble, M. Dagenais, and L. Mandel, Phys. Rev. Lett. **39**, 691 (1977).
[2] P. Horak, B. G. Klappauf, A. Haase, R. Folman, J. Schmiedmayer, P. Domokos, and E. A. Hinds, Phys. Rev. A **67**, 043806 (2003).
[3] A. H. Myerson, D. J. Szwer, S. C. Webster, D. T. C. Allcock, M. J. Curtis, G. Imreh, J. A. Sherman, D. N. Stacey, A. M. Steane, and D. M. Lucas, Phys. Rev. Lett. **100**, 200502 (2008).
[4] T. Bondo, M. Hennrich, T. Legero, G. Rempe, and A. Kuhn, Opt. Commun. **264**, 271 (2006).
[5] N. Lindlein, R. Maiwald, H. Konermann, M. Sondermann, U. Peschel, and G. Leuchs, Laser Phys. **17**, 927 (2007).
[6] G. Shu, N. Kurz, M. R. Dietrich, and B. B. Blinov, Phys. Rev. A **81**, 042321 (2010).
[7] M. K. Tey, G. Maslennikov, T. C. H. Liew, S. A. Aljunid, F. Huber, B. Chng, Z. Chen, V. Scarani, and C. Kurtsiefer, New J. Phys. **11**, 043011 (2009).
[8] P. A. Quinto-Su, M. Tscherneck, M. Holmes, and N. P. Bigelow, Opt. Express **12**, 5098 (2004).
[9] M. Wilzbach, D. Heine, S. Groth, X. Liu, T. Raub, B. Hessmo, and J. Schmiedmayer, Opt. Lett. **34**, 259 (2009).
[10] M. Kohnen, M. Succo, P. G. Petrov, R. A. Nyman, M. Trupke, and E. A. Hinds, Nat. Photonics **5**, 35 (2011).
[11] A. P. Vandevender, Y. Colombe, J. Amini, D. Leibfried, and D. J. Wineland, Phys. Rev. Lett. **105**, 023001 (2010); G. R. Brady, A. R. Ellis, D. L. Moehring, D. Stick, C. Highstrete, *et al.*, arXiv:1008.2977 .
[12] C. Schrama, E. Peik, W. Smith, and H. Walther, Opt. Commun. **101**, 32 (1993).
[13] S. Gulde, D. Rotter, P. Barton, F. Schmidt-Kaler, R. Blatt, and W. Hogervorst, Appl. Phys. B **73**, 861 (2001).
[14] M. Harlander, M. Brownnutt, W. Hänsel, and R. Blatt, New J. Phys. **12**, 093035 (2010).
[15] W. J. Kim, A. O. Sushkov, D. A. R. Dalvit, and S. K. Lamoreaux, Phys. Rev. A **81**, 022505 (2010).
[16] H. J. Carmichael and D. F. Walls, J. Phys. B **9**, 1199 (1976).
[17] F. Diedrich and H. Walther, Phys. Rev. Lett. **58**, 203 (1987).
[18] Y. Colombe, T. Steinmetz, G. Dubois, F. Linke, D. Hunger, and J. Reichel, Nature (London) **450**, 272 (2007).
[19] N. Sangouard, R. Dubessy, and C. Simon, Phys. Rev. A **79**, 042340 (2009).